Conductivity and Magnetic Properties of the Charge-Transfer Complex from N,N′-Dicyanonaphthoquinonedimimine (DCNNI) and Tetrathiafulvalene (TTF)

H.-P. Werner, W. Grauf, J. U. von Schütz, and H. C. Wolf

3. Physikalisches Institut, Universität Stuttgart, West-Germany

H. W. Helberg and W. Kremer

3. Physikalisches Institut, Universität Göttingen, Bürgerstr. 42–44, D-3400 Göttingen, West-Germany

A. Aumüller and S. Hünig

Institut für Organische Chemie, Universität Würzburg, Am Hubland, D-8700 Würzburg, West-Germany

Z. Naturforsch. **44a**, 825–832 (1989); received July 17, 1989

Conductivity (dc and ac), ESR-properties and proton relaxation rates of the charge transfer complex Tetrathiafulvalene – N,N′-dicyanonaphthoquinonediimine in the temperature range between 300 K and 3.8 K are reported. This salt belongs to the unusual group of organic conductors, in which segregated donor and acceptor stacks are associated in a pairwise manner. The physical properties, which are compared with TTF-TCNQ, give evidence of non-stoichiometric charge transfer ($\varrho \neq 1$). A metal like state can be identified for $T > 70$ K, as is seen from the weak temperature dependence of the conductivity ($\sigma_{rt} \approx 30\ \mathrm{Scm}^{-1}$) and the susceptibility ($\chi_{rt} \approx 7.5 \cdot 10^{-4}$ emu/mole) and from the Korringa like temperature dependence of the proton relaxation rates. The drop of the susceptibility at $T_c \approx 70$ K and the activated temperature dependence of the conductivity for $T < 70$ K are explained by a metal-to-semiconductor transition.

1. Introduction

Radical anion salts derived from the TCNQ-like family of acceptors of differently substituted DCNQI's (dicyanoquinonediimines) have recently attracted growing interest, especially when the counterions are metals. $(2,5\text{-DMe-DCNQI})_2Cu$, for example, exhibits at ambient pressure a metallic phase down to the lowest temperatures reached ($T < 10$ K: $\sigma \approx 5 \cdot 10^5\ \mathrm{Scm}^{-1}$) [1]. This remarkable finding can be explained by an enhanced interstack interaction, which results from a higher dimensional molecular overlap of Cu(3d)-orbitals with the $p\pi$-conduction band on the anion stack. All other metallic counterions do not form similar bridges between the organic stacks. These salts therefore can be characterized as 1 d systems, as is seen from their conductivity and from their magnetic properties [2–4]. This low dimensional behaviour exists in DCNQI-salts with organic counterions as well.

Reprint requests to Dr. J. U. v. Schütz, 3. Physikalisches Institut, Universität Stuttgart, Pfaffenwaldring 57, D-7000 Stuttgart 80, West-Germany

In this paper we report on a charge-transfer complex which is built up from N,N′-naphthoquinonediimine (DCNNI) and Tetrathiafulvalene (TTF). A first summary of the physical properties of this compound has already been published [5, 6]. Here we give a more complete set of experimental data because the title compound demonstrates in a special manner which highly conductive organic solids from the DCNQI-family are accessible.

This property depends on the flexibility of the $=N-CN$ groups, which preserves the planarity of the molecule even if bulky substituents are introduced. Planarity of the individual molecules on the other hand favours a stacking arrangement with close intermolecular spacings and therefore allows to form a conduction band of reasonable width. This condition is not satisfied for the TCNQ-analogon of DCNNI. The $-C(CN)_2$-groups are twisted in this case, as is known from crystal structure investigations [7]. Consequently no conducting complex has been isolated so far, whereas TTF-DCNNI shows high conductivity over a wide temperature range.

0932-0784 / 89 / 0900-0825 $ 01.30/0. – Please order a reprint rather than making your own copy.

2. Crystals, Crystal Structure

Shiny black needles of the title compound with a length of up to 10 mm were grown by a reaction of DCNNI and TTF in acetonitrile. The resulting complex exhibits a 1:1 stoichiometry and crystallizes in a monoclinic space group C2/c ($a = 4605.8\,(34)$ pm, $b = 379.6\,(2)$ pm, $c = 2183.4\,(14)$ pm, β 115.76 (1) °, $V = 3.438 \cdot 10^9$ pm^3, ϱ (calc.) = 1.586 gcm^{-1}) [6].

The crystal structure, as shown in Figs. 1 and 2, indicates segregated stacks of equally spaced DCNNI- and TTF-molecules. The distance between neighboring molecules amounts to 353 pm on the TTF-stack and to 329 pm on the DCNNI-stack. These values are only slightly higher than in case of TTF-TCNQ [8] (TTF-stack: 347 pm, TCNQ-stack: 317 pm). But in contrast to TTF-TCNQ, the planes of the TTF and the DCNNI-molecules are tilted by an angle of 9° only. This finding can be attributed to an interaction of the nitrile groups on the DCNNI-molecules with the sulphur-atoms of TTF (see Fig. 1) [6]. This interaction is based on close spacings (323.8 pm and 318.3 pm) between the peripheral nitrogen atoms of DCNNI and the sulphur atoms of two TTF-molecules. As a further consequence of this type of coordination, TTF-DCNNI exhibits a peculiar arrangement of the stacks (Figure 2). Two DCNNI stacks are arranged in such a manner that their "rear sides", which are assumed to be inactive, are adjacent. "In front" of the DCNNI stacks, however, the crystal structure exhibits two parallely aligned TTF stacks. Due to this arrangement of the stacks we expect that the charge carrier transport in TTF-DCNNI is mainly restricted to 1 d columns of strongly coupled donor and acceptor pairs. In this sense, these 1 d columns can be considered as molecular wires.

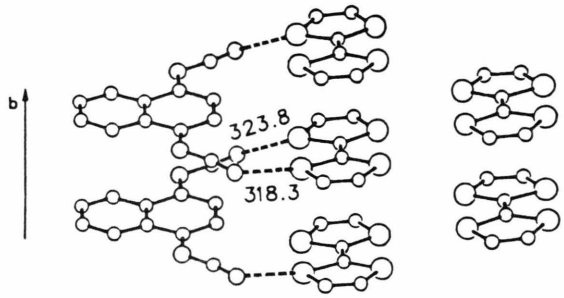

Fig. 1. Intermolecular contacts in TTF-DCNNI [6] (distances in pm).

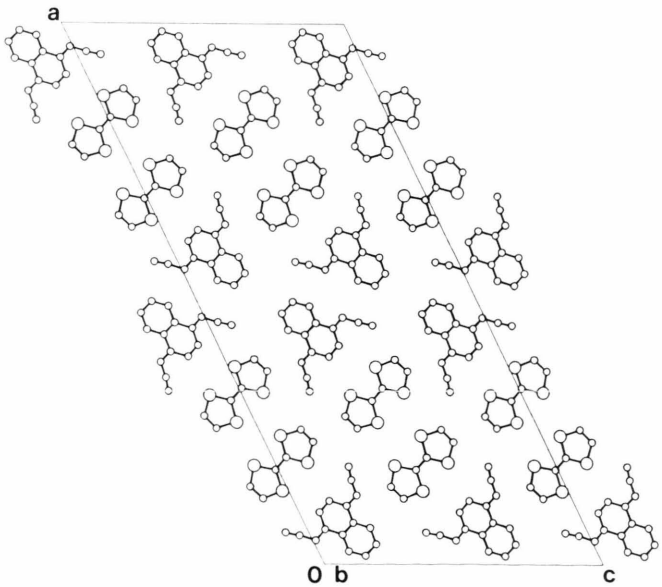

Fig. 2. a/c-projection of the crystal structure [6].

3. Experimental and Results

Conductivity

The dc-conductivity measurements were done by a standard four wire technique with gold paint contacts (Demetron M8001). The ac-conductivity was measured at 10.3 GHz by a cavity perturbation technique [9, 10]. The resulting room temperature conductivities range from 20–30 Scm^{-1}. The temperature dependent dc-conductivities and ac-data of two samples are given in Figure 3.

During thermal cycling of the crystals we always observed sudden jumps of the dc-resistivity (mainly in the temperature range 150–100 K). In analogy to similar findings in the literature [11], they are attributed to cracks, the more as they are accompanied by a large hysteresis on the heating run and by a decreased room temperature conductivity. Therefore the $\sigma(T)$-data given in Fig. 3 are corrected for these jumps. The corrected data closely follow σ_{ac} down to 70 K and can be characterized as follows: From 300 K down to 130 K σ_{dc} increases by 30%. Below 130 K there appears a gradual transition into a semiconducting state, resulting in an activation energy of $\Delta(\sigma_{dc}) = (0.07 \pm 0.01)$ eV below 70 K. In the latter range σ_{ac} and σ_{dc} differ ($\Delta(\sigma_{ac}) \approx 0.015$ eV).

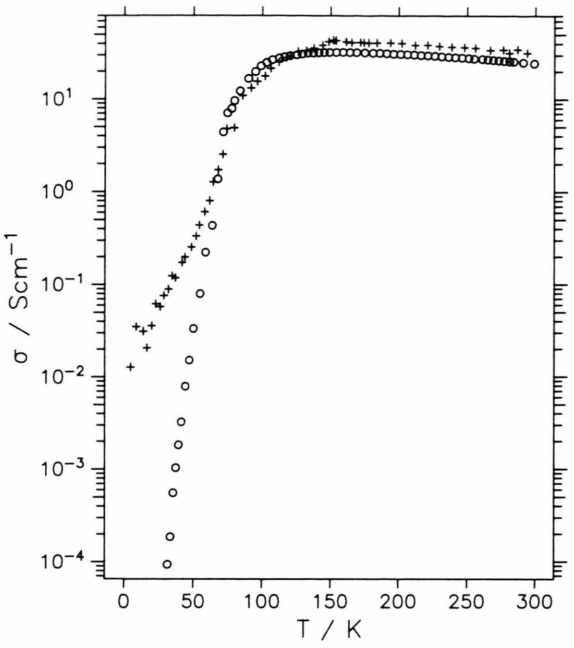

Fig. 3. Temperature dependence of the electrical conductivity of TTF-DCNNI: Crosses: ac-conductivity at 10.3 GHz; open circles: corrected dc-data (see text).

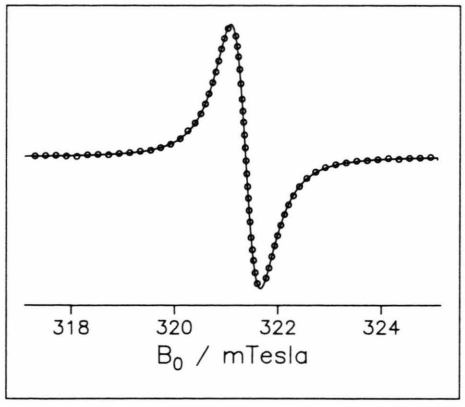

Fig. 4. ESR-spectrum (derivative) at room temperature: Open circles: observed ESR-line; solid line: calculated Lorentzian ESR-line.

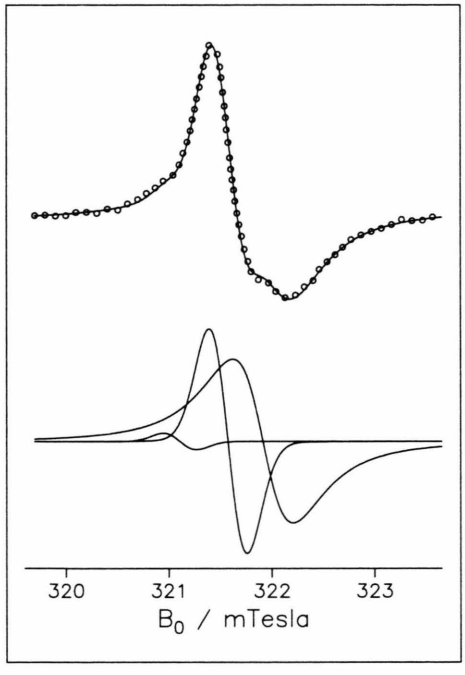

Fig. 5. Top: ESR-line (derivative) observed at 10 K for $B_0 \| y$ (open circles) and calculated ESR-line (solid line). Bottom: Components of the calculated ESR-line.

ESR

The ESR-experiments were performed in a conventional Varian-Century-line E-109 spectrometer, equipped with an Oxford ESR-9 helium flow-cryostat which was used also for the dc-conductivity measurements. The paramagnetic susceptibility was calculated from the ESR intensity by calibration with the signal intensity of a standard ruby sample (NBS-SRM 2601). Temperature dependent changes of the quality factor of the cavity were monitored and corrected by comparison with the known Curie-like susceptibility of the standard ruby.

In the temperature range of 300–50 K, the ESR spectra of thin samples ($d < 100$ μm) consisted of a single Lorentzian shaped line (Figure 4). Above 100 K, in the region of high conductivity, a Dysonian lineshape was found for certain orientations of thicker samples. Below 50 K, the signal became asymmetric for all samples. In the orientation of the highest g-value the ESR-line can be fit by three single lines (Figure 5).

The principal values of the linewidth ΔB_{pp} and the g-tensor at room temperature are listed in Table 1. The minimum g-value and ESR linewidth is found

Table 1. Principal values (300 K and 70 K) of the ESR linewidth and the g-Tensor.

	g		ΔB_{pp}	
	300 K	70 K	300 K	70 K
$B_0 \| z$	2.0034	2.0034	0.38	0.67
$B_0 \| x$	2.0063	2.0067	0.41	0.69
$B_0 \| y$	2.0074	2.0084	0.60	1.15

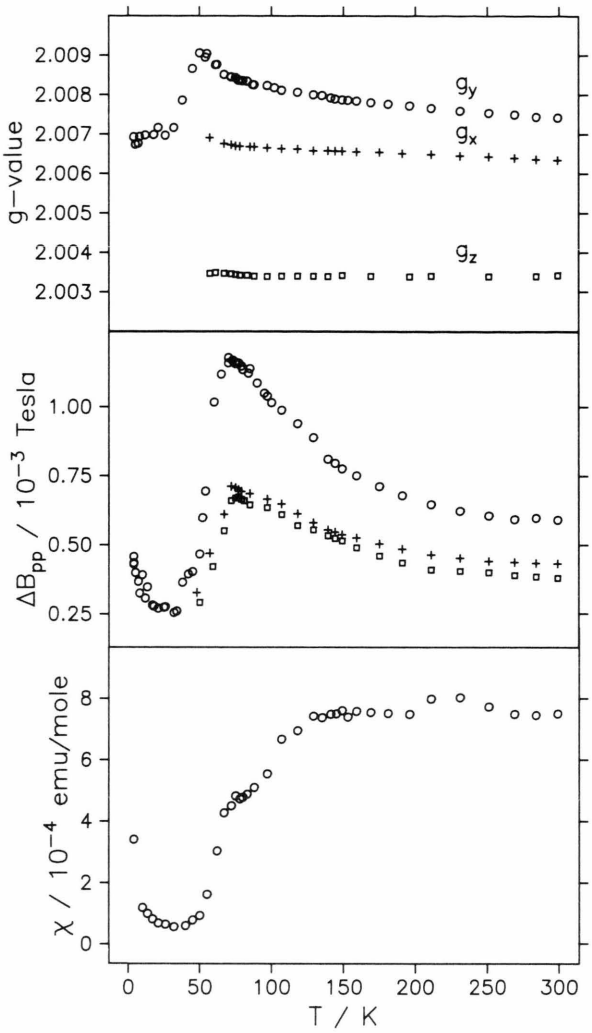

Fig. 6. ESR-results: g-value, linewidth and susceptibility as a function of temperature. The linewidth and the g-value data for $T < 50$ K represent the results of the fits for the central line of Fig. 5. (bottom).

for $B_0 \| z$ (stacking axis). The intermediate and the highest component of the g-tensor (and ΔB_{pp} as well) lie in the a, c-plane (x- and y-direction). The isotropic g-value amounts to 2.0057 ± 0.0002 at 300 K and to 2.0062 ± 0.0002 at 70 K.

The T-dependent ESR-data (g-value, linewidth and susceptibility) are plotted in Figure 6. Below 50 K the g-value and linewidth-data are shown for the orientation of maximum g-value only. They were obtained from the fits by three single lines, as mentioned above.

Two components of the g-tensor are temperature dependent. This temperature dependence is most pronounced for $B_0 \| y$. In this orientation, g_y reaches a maximum at 50 K, just at the temperature where the lineshape becomes asymmetric. Below 50 K, the g-value of the central line starts to decrease from this maximum value, as is deduced from the fits with three lines. The other two lines correspond to g-values of 2.0105 (5) and 2.0050 (5).

In all three principal orientations the linewidth significantly broadens with decreasing temperature, reaching a maximum at ≈ 70 K. Below 70 K the linewidth components drop within 20 K by a factor of two. Below 20 K the asymmetric signal broadens again.

The ESR-susceptibility is roughly constant down to 130 K ($7.5 \cdot 10^{-4}$ emu/mole). Then χ starts to decrease, to exhibit a sharp drop at ca. 70 K, in the same temperature range where the linewidth begins to decrease. Below 20 K we find a $1/T$ increase of the susceptibility. This contribution is sample dependent and corresponds roughly to $\approx 2 \cdot 10^{21}$ mole^{-1} of paramagnetic states obeying Curie's law.

NMR

A home built spectrometer was used for pulsed NMR experiments at 22 and 44 MHz. T_{1H}^{-1} proton relaxation rates on samples with deuterated and undeuterated acceptors were measured by observing the time recovery of the free induction decay after a saturation pulse sequence. Above 70 K, the relaxation rates are frequency dependent and exhibit a T^{-1} temperature dependence. The results at 44 MHz are given in Figure 7. In the temperature range in which the T^{-1}-law holds, we found similar relaxation rates for the deuterated sample as for the undeuterated one. The peak in T_{1H}^{-1}, which is seen at about 30 K is much less pronounced in case of deuterated samples.

4. Discussion

Conductivity

Although the crystal structure exhibits similar characteristics as TTF-TCNQ (segregated stacks, close intrastack spacings), the conductivity of TTF-DCNNI differs considerably from that of the latter salt. The room temperature conductivity of TTF-DCNNI is an order of magnitude lower and the T-dependence in the conducting range is very weak, showing a broad maximum at 150 K.

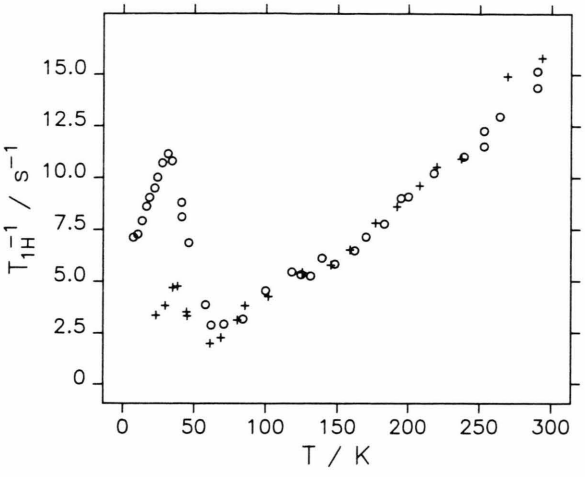

Fig. 7. Proton relaxation rates at 44 MHz as a function of temperature (crosses: DCNNI deuterated; open circles: undeuterated sample).

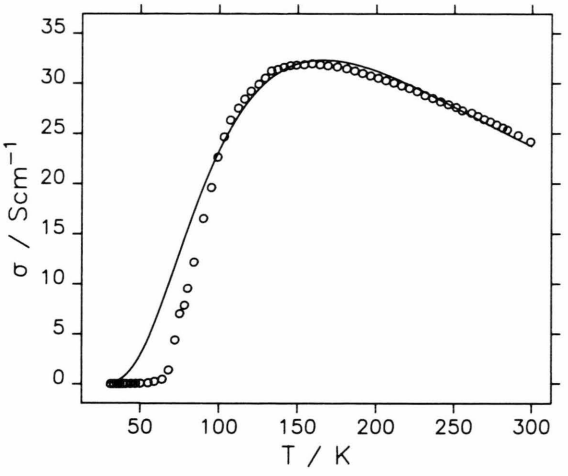

Fig. 8. Comparison of $\sigma_{dc}(T)$ with the calculated T-dependence according to (1) ($\alpha = 2.15$, $\Delta_H = 0.03$ eV).

Such characteristic features are found for many low dimensional organic conductors and can be explained by several limiting factors concerning the transport properties in the 1 d case: i. e. localization of the charge carriers by defects within the molecular stacks [13], by electron-electron correlations, which, if the Coulomb repulsion U between electrons on the same molecule is strong enough, can localize the electrons by opening a gap at the Fermi-level for $\varrho = 0.5$ [14] and for $\varrho = 1$ [13] (ϱ: charge density per molecular unit). Finally, as a consequence of electron-phonon coupling, 1 d systems exhibit an instability against lattice distortions, which result in metal insulator transitions [15]. These phase transitions are often accompanied by fluctuations, which can appear over a wide temperature range above the actual phase transition temperature T_c. Such a coupled electron-phonon system can be described as a charge density wave (CDW) with finite coherence length, which can be pinned by defects or by commensurability with the lattice constant ($\lambda_{CDW} = n\,b$; $n = 1, 2, 3, \ldots$; b: lattice constant). In the non commensurable case sliding CDW's might contribute to the conductivity, dominating the T-dependence of $\sigma(T)$ in case of TTF-TCNQ [16]. Apparently such a contribution is not present for TTF-DCNNI, as is deduced from the lack of a pronounced conductivity peak.

The $\sigma(T)$-curve of TTF-DCNNI can be approximated by a phenomenological model proposed by Epstein et al. [13]. In this model the mobility is assumed to be strongly T-dependent ($\mu \sim T^{-\alpha}$; α: sample dependent constant), and the concentration of mobile charge carriers is assumed to be thermally activated, resulting in

$$\sigma(T) = A \cdot e^{-\Delta_H/kT} \cdot T^{-\alpha}. \tag{1}$$

In Fig. 8, the solid line is the best fit to (1) with $\Delta_H = 0.03$ eV and $\alpha = 2.15$. There is some discrepancy in T_m (temperature of the conductivity maximum) between the experimental and the calculated $\sigma(T)$ data. This discrepancy, however, is not surprising, since both stacks with (different) individual T-dependences might contribute to the measured conductivity.

Below 70 K, the deviation of the calculated $\sigma(T)$-curve from the experimental data is even more pronounced. Here we find an increased activation energy of $\Delta_L(\sigma_{dc}) \approx 0.07$ eV. This is a clear indication for a structural phase transition. In the same temperature range σ_{ac} exhibits a considerably weaker T-dependence than σ_{dc}. The origin of this excess conductivity at high frequencies is unknown so far but could be explained by a collective charge transport mechanism in small dimensions [17].

Susceptibility

Concerning the magnetic properties, the differences between TTF-TCNQ and the title compound are much less pronounced. The room temperature susceptibility of TTF-DCNNI is slightly higher (ca. 25%),

giving evidence of reasonable Coulomb interactions. In the picture of non interacting electrons (Pauli susceptibility), the room temperature susceptibility of $7.5 \cdot 10^{-4}$ emu/mole would result in a bandwidth of $4t_{\|} < 0.1$ eV, assuming a charge transfer $\varrho \approx 0.6$ as found for TTF-TCNQ [16]. Such a small bandwidth should give rise to a considerable T-dependence of the susceptibility, in contradiction to the experimental results, as $\chi(T)$ is almost constant down to 130 K, therefore justifying the introduction of U. The gradual decrease of χ below 130 K can be explained by precursor effects of the phase transition at $T_c \approx 70$ K, which seem to affect mainly the density of states on the DCNNI stack, as will be shown later.

After subtraction of the Curie contribution, the product χT gives an activation energy on the order of ≈ 0.01 eV for $T < 70$ K. This value is considerably lower than the activation energy Δ_L deduced from the conductivity in this temperature range. This is a further indication of considerable Coulomb interactions, since in that case the spin- and charge carrier excitations become decoupled. In the limit of large U, the spin- and charge excitations have different periods and their gaps will be caused by different distortions [12]. Under that aspect, the χT activation energy would indicate a spin-wave energy gap of $\Delta_{sp}(\chi) \approx 0.01$ eV. In contrast, the σ activation energy would correspond to an energy gap of $2\Delta_L(\sigma) \approx 0.14$ eV, since the charge carrier excitations are fermions. In the presence of defects, the observed dc-conductivity could decrease faster than χT as well, if the conductivity along the stacks is severely limited by insulating barriers (hopping model).

ESR-Lineshape and g-Value

Single chain conductors of substituted DCNQI's (with the exception of Iodine substituted DCNQI's), like the alkaline (Li, Na, K) salts [3] or (2,5-DCl-DCNQI)$_2$N(CH$_3$)$_4$ [18] for example, all exhibit isotropic g-values $\bar{g}$ close to 2.0044. For the DCNNI stack we expect $\bar{g}_A$ to be similar to those, as DCNNI does ot contain heavy heteroatoms like S or Se, which considerably enhance spin-orbit coupling. On the other hand, as is known from the halides of TTF [19] and from measurements of TTF^+ in solution [20], $\bar{g}_D$ of the donor chain is expected to be ≈ 2.0083. Actually we find a single Lorentzian absorption line at an intermediate g-value of $\bar{g} = 2.0057$ (at 300 K), which demonstrates that both stacks contribute to the magnetic properties. The interstack hopping rate of spin excitations, however, must be faster than the difference between the respective Larmor frequencies on the donor and the acceptor stack, otherwise two absorption lines should be observed. In the strong coupling limit the averaged g-value then depends on the individual donor and acceptor stack susceptibilities χ_D and χ_A by the equation [12]

$$g = g_A(\chi_A/\chi_T) + g_D(\chi_D/\chi_T) \quad \text{with } \chi_T = \chi_D + \chi_A. \quad (2)$$

Under the condition of temperature independent g-values of the individual components, (2) often allows to analyse the fractional susceptibilities on both kind of stacks [12, 21, 22]. We dont want to perform such a quantitative analysis but some qualitative remarks can be made in spite of the fact that there is some uncertainty in the precise value of $\bar{g}_A$.

The isotropic g-value continuously increases from 300 K down to 50 K. This temperature dependence is most pronounced in the phase transition region (below 130 K), as is seen from the slope of $g_y(T)$. We attribute this finding to a decreasing DCNNI stack contribution to χ_T. The stronger T-dependence of the g-value below 130 K and the beginning decrease of the susceptibility gives further hints for precursor effects of the phase transition, which seem to affect mainly the density of states on the acceptor stack. As this trend is enhanced below $T_c \approx 70$ K, we have to assume that the gap, which is opened at T_c, is broader on the DCNNI stack.

The trend of the g-shift as a function of decreasing temperature reverses just at that temperature ($T = 50$ K) at which the signal splits in three barely resolved absorption lines. We attribute these partially resolved signals to localized spins on the TTF and DCNNI stacks, which may be introduced by stack interruptions, for example. These spins are only weakly coupled, as is seen from the Curie like increase of the susceptibility at the lowest temperatures, and consequently averaging of their individual g-values is not complete anymore. Some of these localized spins, however, are close enough for interchain coupling, resulting in the central line of Figure 5. From the T-dependent g-value of this central line and from the weakness of the signal on the high g-value side (TTF), we have to conclude that most of these crystalline imperfections are situated on the DCNNI stack.

ESR-Linewidth

The temperature dependence of the ESR-linewidth (in the conducting range), as shown in Fig. 6, is differ-

ent from the results on single chain conductors of substituted DCNQI's. The corresponding Ag-salts, for example, exhibit a decreasing linewidth with decreasing temperature [2]. From angle dependent measurements of the g-value and the ESR-linewidth on these Ag-salts we have deduced that their dominant spin-relaxation mechanism is mediated by spin-orbit coupling [2]. The same mechanism, however, must be responsible for the ESR-linewidth of TTF-DCNNI. As is expected in this case, we find the minima and maxima of the linewidth and g-value for the same orientations (in respect to B_0) of the crystal (see Table 1).

In 1 d systems, spin relaxation by spin-orbit coupling depends on the g-shift of the ESR-line and on the interstack scattering time $\tau_\perp$. According to the modified Elliot relation the linewidth then reads [16] $1/T_2 \sim (\Delta g^2/\tau_\perp)$. In comparison to our experimental data, the increase of the g-shift $(\Delta \bar{g}^2)$ by 30% on cooling from 300 K to 70 K cannot solely explain $\Delta B_{pp}(T)$, which in the same range increases by more than 70%. This discrepancy gives evidence of an enhancement of interstack interactions on cooling, which results in a decrease of $\tau_\perp$. In the same model, the drop of the linewidth below 70 K is explained by the opening of a gap in the density of states at the Fermi level [16].

Proton Relaxation Rates

The metal like character of TTF-DCNNI above 70 K is confirmed by the temperature dependence of T_{1H}^{-1}, as our experimental data closely follow a Korringa law $T_{1H} T \chi^2 = \text{const}$, which results from the interaction of the protons with the mobile charge carriers. Of importance is the fact that we find the same relaxation rates for the deuterated and the undeuterated sample in this range. This finding shows that both stacks contribute to the physical properties and that we have to deal with similar concentrations of delocalized charge carriers on the TTF and the DCNNI stacks.

Below T_c, $T_{1H}^{-1}(T)$ is similar to the values for the radical anion salts of substituted DCNQI's with metallic counterions. For these salts, peaks of T_{1H}^{-1} at 30 K with comparable magnitude were observed too. Due to their sensitivity to the impurity concentration, they were attributed to an interaction of the protons with localized paramagnetic centers [4]. The relaxation times of those are given by the coupling to "free" spins with temperature dependent concentration. If we adopt this interpretation to the TTF-DCNNφI peaks, it is obvious that the concentration of these centers is considerably lower on the TTF-stack (in agreement with the interpretation of the ESR-data below 50 K), as is seen from comparison of the peak amplitudes of the deuterated (DCNNI) and the undeuterated sample.

Conclusions

By comparison of the physical properties of the title compound and TTF-TCNQ it can be concluded that the magnetic properties of TTF-DCNNI result from contributions of both the acceptor and the donor stacks, as is the case for TTF-TCNQ.

The differences concerning the absolute values and the temperature dependencies of the conductivity between these two charge transfer salts can be attributed to a more pronounced 1 d character of TTF-DCNNI, as it is suggested from the crystal structure that the charge carrier propagation is restricted to weakly interacting columns of strongly coupled donor and acceptor stacks. A charge transfer closer to the commensurate value $\varrho = 0.5$ might provide a further explanation for the lower conductivity of this salt. Under this assumption an enhancement of Coulomb interactions is expected [23] which can induce a localization of the charge carriers and, as confirmed experimentally, increase the susceptibility. Finally, a charge transfer of $\varrho \approx 0.5$ would easily explain the lack of a pronounced conductivity peak by pinning of the CDW's due to commensurability of the CDW-wavelenght and the lattice, but this point needs further experimental verification (X-ray diffuse scattering).

Acknowledgement

This work was supported by the Stiftung Volkswagenwerk.

[1] A. Aumüller, P. Erk, G. Klebe, S. Hünig, J. U. von Schütz, and H.-P. Werner, Angew. Chemie **98,** 159 (1986); Angew. Chemie Int. Ed. Engl. **25,** 740 (1986).
[2] H.-P. Werner, J. U. von Schütz, H. C. Wolf, R. Kremer, M. Gehrke, A. Aumüller, P. Erk, and S. Hünig, Solid State Comm. **65,** 809 (1988).
[3] J. U. von Schütz, M. Bair, H. J. Gross, U. Langohr, H.-P. Werner, H. C. Wolf, D. Schmeißer, K. Graf, W. Göpel, P. Erk, H. Meixner, and S. Hünig, Synth. Metals **27,** 249 (1988).
[4] J. U. von Schütz, M. Bair, U. Langohr, H.-P. Werner, H. C. Wolf, P. Erk, and S. Hünig, Springer Series of Solid State Sciences, June 1989.
[5] W. Grauf, A. Schätzle, J. U. von Schütz, H. C. Wolf, A. Aumüller, and S. Hünig, 22nd Congress Ampere Proceedings, Zürich 1984.
[6] A. Aumüller, E. Hädicke, S. Hünig, A. Schätzle, and J. U. von Schütz, Angew. Chemie **96,** 439 (1984).
[7] F. Iwasaki, Acta Cryst. **B27,** 1360 (1971).
[8] T. J. Kistenmacher, T. E. Phillips, and D. O. Cowan, Acta Cryst. **B30,** 763 (1974).
[9] H. W. Helberg and B. Wartenberg, Z. Angew. Phys. **20,** 505 (1966).
[10] H. Schäfer and H. W. Helberg, Phys. Stat. Sol. (a) **63,** 203 (1981).
[11] C. Coulon, P. Delhaes, S. Flandrois, R. Lagnier, E. Bonjour, and J. M. Fabre, J. Physique **43,** 1059 (1982).
[12] Y. Tomkiewicz, A. R. Taranko, and J. B. Torrance; Phys. Rev. **B15,** 1017 (1977).
[13] A. J. Epstein and E. M. Conwell, Solid State Comm. **24,** 627 (1977).
[14] K. Holczer, G. Mihaly, A. Janossy, and G. Gruner, Mol. Cryst. Liq. Cryst. **342,** 199 (1976).
[15] R. E. Peierls, Quantum Theory of Solids, Osxford University Press, London 1955.
[16] D. Jerome and H. J. Schulz, Adv. Physics **31,** 299 (1982).
[17] G. J. Kramer, J. L. Joppe, H. D. Brom, L. J. De Jongh, and J. L. De Boer; Synth. Metals **19,** 439 (1987).
[18] H.-P. Werner, J. U. von Schütz, H. C. Wolf, R. Kremer, M. Gehrke, A. Aumüller, P. Erk, and S. Hünig, Solid State Comm. **69,** 1127 (1989).
[19] Y. Tomkiewicz, F. Mehran, D. C. Green, and B. A. Scott, Bull. Amer. Phys. Soc. **19,** 334 (1974).
[20] F. Wudl, G. M. Smith, and E. J. Hufnagel, J. Chem. Soc. D **1970,** 1453.
[21] Y. Tomkiewicz, A. R. Taranko, and R. Schumaker, Phys. Rev. **B16,** 1380 (1977).
[22] Y. Tomkiewicz, J. R. Andersen, and A. R. Taranko, Phys. Rev. **B17,** 1579 (1978).
[23] S. Mazumdar and A. N. Bloch, Phys. Rev. Lett. **50,** 207 (1983).